of cell-cell contact where membrane-cytoskeletal complexes are assembled, possibly by linkage to E-cadherin (*23*) (Fig. 1). In membranes that lack membrane-cytoskeletal complexes (such as the apical membrane of MDCK cells) Na^+, K^+-ATPase is rapidly internalized at a rate (Fig. 4) similar to that of constitutive endocytosis of cell surface markers (~2 hours) (*23*). Assembly of the membrane-cytoskeletal complexes in selective domains may provide a flexible mechanism for generating different distributions of Na^+, K^+-ATPase in other polarized epithelial cells in which the same subunits are localized to the apical membrane (*1, 2*) or to both (*4*) the apical and lateral membranes.

REFERENCES AND NOTES

1. E. M. Wright, *J. Physiol.* **226**, 545 (1972); W. L. Stahl, *Neurochem. Int.* **8**, 449 (1986); J. A. Marrs, R. W. Mays, W. J. Nelson, *J. Am. Soc. Nephrol.* **1**, 711 (1990).
2. S. Ghosh, A. C. Freitag, P. Martin-Vasallo, M. Coca-Prados, *J. Biol. Chem.* **265**, 2935 (1990); D. Gunderson, J. Orlowski, E. Rodriguez-Boulan, *J. Cell Biol.* **112**, 863 (1991).
3. M. Kashgarian, D. Biemesderfer, M. Caplan, B. Forbush III, *Kidney Int.* **28**, 899 (1985); K. J. Sweadner, *Biochim. Biophys. Acta* **988**, 185 (1989).
4. P. D. Wilson *et al.*, *Am. J. Physiol.* **260**, F420 (1991); E. Avner, W. Sweeney, W. J. Nelson, in preparation.
5. B. Molitoris *et al.*, *J. Membr. Biol.* **106**, 233 (1988).
6. E. Rodriguez-Boulan and W. J. Nelson, *Science* **245**, 718 (1989).
7. K. Simons and S. D. Fuller, *Annu. Rev. Cell Biol.* **1**, 243 (1985); M. Caplan and K. S. Matlin, in *Modern Cell Biology*, B. Satir, Ed. (Liss, New York, 1989), vol. 8, pp. 71–127; A. L. Hubbard, J. R. Bartles, B. Steiger, *Annu. Rev. Physiol.* **51**, 755 (1989).
8. P. Ekblom, D. Vestweber, R. Kemler, *Annu. Rev. Cell Biol.* **2**, 27 (1986).
9. W. J. Nelson and P. J. Veshnock, *J. Cell Biol.* **104**, 1527 (1987).
10. G. K. Ojakian and R. Schwimmer, *ibid.* **107**, 2377 (1988).
11. M. Sargiacomo, M. Lisanti, L. Graeve, A. LeBivic, E. Rodriguez-Boulan, *J. Membr. Biol.* **107**, 277 (1989); K. Matter, M. Braucher, K. Bucher, H.-P. Hauri, *Cell* **60**, 429 (1990).
12. R. Bacallao *et al.*, *J. Cell Biol.* **109**, 2817 (1989).
13. D. Wollner, K. A. Krzeminski, W. J. Nelson, in preparation.
14. M. Pasdar and W. J. Nelson, *J. Cell Biol.* **109**, 163 (1989); S. M. Cohen, G. Gorbsky, M. S. Steinberg, *J. Biol. Chem.* **258**, 2621 (1983).
15. M. J. Caplan, H. C. Anderson, G. E. Palade, J. D. Jamieson, *Cell* **46**, 623 (1986).
16. P. L. Jorgensen, *Biochim. Biophys. Acta.* **694**, 27 (1982).
17. R. G. Contreras *et al.*, *Am. J. Physiol.* **257**, C896 (1989).
18. R. W. Hammerton, K. A. Krzeminski, R. W. Mays, T. A. Ryan, D. A. Wollner, W. J. Nelson, unpublished data.
19. K. Simons and G. van Meer, *Biochemistry* **27**, 6197 (1988).
20. R. A. Kelly, D. S. O'Hara, W. E. Mitch, T. W. Smith, *J. Biol. Chem.* **261**, 11704 (1986). B. Zheng, *et al.*, *Cancer Res.* **50**, 3025 (1990); E. Sutherland *et al.*, *Proc. Natl. Acad. Sci. U.S.A.* **85**, 8673 (1988).
21. W. J. Nelson and P. J. Veshnock, *Nature* **328**, 533 (1987): J. S. Morrow, C. D. Cianci, T. Ardito, A. S. Mann, M. Kashgarian, *J. Cell Biol.* **108**, 455 (1989). W. J. Nelson and R. W. Hammerton, *ibid.*, p. 893; R. Koob, M. Zimmerman, W. Schoner, D. Drenckhahn, *Eur. J. Cell Biol.* **45**, 230 (1987).
22. W. J. Nelson, E. S. Shore, A. Z. Wang, R. W. Hammerton, *J. Cell Biol.* **110**, 349 (1990).
23. H. McNeill, M. Ozawa, R. Kemler, W. J. Nelson, *Cell* **62**, 309 (1990).
24. C.-H. von Bonsdorf, S. D. Fuller, K. Simons, *EMBO J.* **4**, 2781 (1985).
25. H. Towbin, T. Staehlin, J. Gordon, *Proc. Natl. Acad. Sci. U.S.A.* **76**, 4350 (1979).

26. T.A.R. thanks S. Smith for support and encouragement. Supported by grants from the NIH (GM 35527) March of Dimes Foundation (W.J.N.) by a National Kidney Foundation postdoctoral fellowship (R.W.H.) and a postdoctoral fellowship from the NIH (D.W.). W.J.N. is an Established Investigator of the American Heart Association.

11 March 1991; accepted 7 August 1991

Activation of a Small GTP-Binding Protein by Nucleoside Diphosphate Kinase

PAUL A. RANDAZZO, JOHN K. NORTHUP, RICHARD A. KAHN*

Genes that encode nucleoside diphosphate kinases (NDKs) have been implicated as regulators of mammalian tumor metastasis and development in *Drosophila melanogaster*. However, the cellular pathways through which NDKs function are not known. One potential mechanism of regulation is phosphorylation of guanosine diphosphate (GDP) bound to regulatory guanosine triphosphate (GTP) binding proteins. NDK-catalyzed phosphorylation of bound GDP was investigated for the adenosine diphosphate ribosylation factor (ARF), a 21-kilodalton GTP-binding protein that functions in the protein secretion pathway. Bovine liver NDK, recombinant human NDK, and the protein product of the mouse gene nm23-1, which suppresses the metastatic potential of certain tumor cells, used ARF·GDP as a substrate, thereby allowing rapid and efficient production of activated ARF (ARF·GTP) in the absence of nucleotide exchange. These data are consistent with the proposed function of NDK as an activator of a small GTP-binding protein and provide a mechanism of activation for a regulatory GTP-binding protein that is independent of nucleotide exchange.

NUCLEOSIDE DIPHOSPHATE KINASE (NDK) is a commonly occurring enzyme that catalyzes the phosphorylation of nucleoside diphosphates by nucleoside triphosphates. The NDKs have been proposed to function in the maintenance of nucleoside triphosphate pools (*1, 2*). Cloning of two genes encoding homologs of NDK, nm23, (expression of which reduces the metastatic potential of certain tumor cells) and awd (a developmental gene) (*3*), has renewed previous speculation (*2*) that NDKs may serve regulatory functions. One possible site of NDK action is as an activator of regulatory guanine nucleotide-binding proteins. If NDK serves as an activator of a regulatory GTP-binding protein the enzyme must utilize GDP as a substrate while GDP is bound to the regulatory protein, and the NDK-catalyzed production of GTP must result in activation of the regulatory protein. Several regulatory GTP-binding proteins, including members of both the heterotrimeric G protein family and the monomeric 20- to 25-kD family, have been examined as potential NDK substrates (*4, 5*). However, it has not been shown that NDK can use bound GDP as a substrate or that a GTP-binding protein can be activated by such a mechanism. ADP ribosylation factor (ARF), a 21-kD GTP-binding protein implicated in Golgi function, has two characteristics that helped us to examine these issues. First, the activity of ARF can be assessed with a simple in vitro assay, that is, ARF is a required cofactor for the cholera toxin–catalyzed ADP ribosylation of G_s, a heterotrimeric G protein (*6, 7*). This activity is found only for GTP-bound ARF and not the GDP-bound protein. Second, nucleotide exchange kinetics of the purified protein have been well characterized, and in the absence of phospholipid and detergent the nucleotide dissociation rate is negligible (*7*). Even under optimal conditions for nucleotide exchange the release of GDP is slow and the stoichiometry of GTP binding is less than 0.10.

Addition of NDK to purified ARF that was first bound with [α-^{32}P]GDP caused conversion to [α-^{32}P]GTP at a rate proportional to the quantity of added NDK (Fig. 1A) (*8*). At the highest concentration of NDK examined (140 nM), 80% of the bound GDP was converted to GTP within 3 min (*9*). We obtained similar results using commercially available bovine liver NDK or purified recombinant nm23-H1, nm23-H2, or nm23-1 proteins (*10, 11*). Our results

P. A. Randazzo and R. A. Kahn, Laboratory of Biological Chemistry, Division of Cancer Treatment, National Cancer Institute, Bethesda, MD 20892.
J. K. Northup, Department of Pharmacology, Yale University School of Medicine, New Haven, CT 06514.

*To whom correspondence should be addressed.

(Fig. 1) appear to represent a single exponential process. When the kinetics of GTP formation from ARF·GDP were examined, the rate saturated hyperbolically as a function of the concentration of ARF·GDP (Fig. 1B). Hence, we compared the substrate activity of ARF·GDP and GDP (*12*). Using the nm23-H1 NDK, we determined the $K_{m,app}$ and $V_{max,app}$ to be 0.16 ± 0.05 μM and 5.1 ± 0.4 μmol/min per milligram of protein for ARF·GDP as a substrate, and 37 ± 3.5 μM and 210 ± 15 μmol/min per milligram of protein for free GDP as a substrate. Thus, the affinity of NDK for ARF·GDP is about 200 times greater than that for free GDP, and the rate of phosphorylation of GDP is 40 times that of ARF·GDP. This relatively high affinity of NDK for ARF·GDP suggests the formation of a stable complex that may serve to modulate the activity of one or both proteins.

Phosphorylation of ARF·GDP occurs in the absence of nucleotide exchange, suggesting that ARF·GDP, rather than free nucleotide, is the substrate for NDK. No exchange of nucleotide was detected when [α-^{32}P]GDP-bound ARF was incubated with an excess of unlabeled GDP (1000 times more) in the absence of phospholipid (Fig. 1C) (7). Similarly, no binding of [γ-^{32}P]GTP to ARF was detected in the absence of phospholipid (Fig. 1C). Under optimal conditions for exchange (7) less than 8% of ARF was converted to the GTP bound form after 1 hour at 30°C (Fig. 1C). Hence, guanine nucleotide exchange cannot account for the rapid and efficient production of ARF·GTP by NDK. As a further test of this conclusion, an excess of unlabeled GTP (1000 times more) was included in the NDK reaction mixture, which contained [α-^{32}P]GDP·ARF, and ^{32}P bound to ARF was measured. During conversion of bound GDP to GTP, dilution of the radioisotope bound to ARF was not observed; dilution would be expected if nucleotide exchange had occurred (Fig. 1C). Furthermore, when the samples were fractionated on Sephadex G-25 resin, all label was recovered in the void volume along with ARF; none was recovered in the fraction that contained free nucleotide (*10*). These data demonstrate that protein-bound GDP was rapidly and efficiently phosphorylated in the absence of nucleotide exchange.

Addition of human (nm23-H1) (Fig. 2), murine (nm23-1) (Fig. 2), or bovine (liver) (*5, 10*) NDKs to the ARF assay resulted in an accelerated rate of cholera toxin–catalyzed ADP ribosylation of G_s. In that ARF·GTP, and not ARF·GDP, has been shown to be the active species in the cholera toxin–catalyzed reaction (*6, 7*), these results are consistent with the NDK-catalyzed production of ARF·GTP. We considered two other interpretations of the data to be less likely. (i) NDK may serve as a GTP regenerating system to maintain GTP concentrations, thus resulting in higher ARF activity. Hydrolysis of GTP in the ARF assay (*13*) was found to be very slow [<1% of the GTP (originally present at 100 μM) or <2% of the GTP (originally present at 20 μM) was hydrolyzed after 150 min at 30°C] and, thus, regeneration of GTP by the inclusion of NDK and ATP cannot account for the observed activities. (ii) G_s·GDP may be a substrate for NDK and in the GTP-bound form serve as a better substrate for cholera toxin–catalyzed ADP ribosylation. Because of the participation of two GTP-binding proteins in this reaction, it has proven difficult to clearly resolve effects of nucleotides on the individual regulatory proteins. It is conceivable that NDK phosphorylates G_s·GDP like it does ARF·GDP and that the G_s·GTP so formed is a better substrate for ADP ribosylation by cholera toxin. However, the ADP ribosylation reaction is dependent on ARF and activation of ARF with hydrolysis-resistant GTP analogs can relieve the guanine nucleotide requirement of the reaction (7). Hence, our data indicate that NDK can activate ARF. We propose that the phosphorylation of ARF·GDP to form ARF·GTP results in the attainment of its active conformation. The conformation of ARF·GTP produced by NDK was independently determined by a second means (*14*). ARF·GTP binds to phospholipid vesicles and sediments more rapidly in sucrose gradients than ARF·GDP, which does not bind the vesicles and sediments at a rate consistent with it being a 21-kD monomer. Addition of NDK and ATP to ARF before the mixture was placed on sucrose gradients was sufficient to promote association of ARF with phospholipid vesicles in the absence of any added GTP (*10*). This result confirms the conclusion that the ARF·GTP produced by NDK is indeed an activated species of ARF.

The ability to produce ARF·GTP without the need of either phospholipid or free GTP should prove useful for the examination of the in vitro properties of ARF and its roles in cholera toxin–catalyzed ADP ribosylation and protein secretion. Our experiments (Fig. 2) have revealed that phospholipid is required for ADP ribosylation at a step distal to the activation of ARF. These results also show that GTP is required in the cholera toxin reaction at a step subsequent to activation of ARF, because no ADP ribosylation was observed in the absence of added

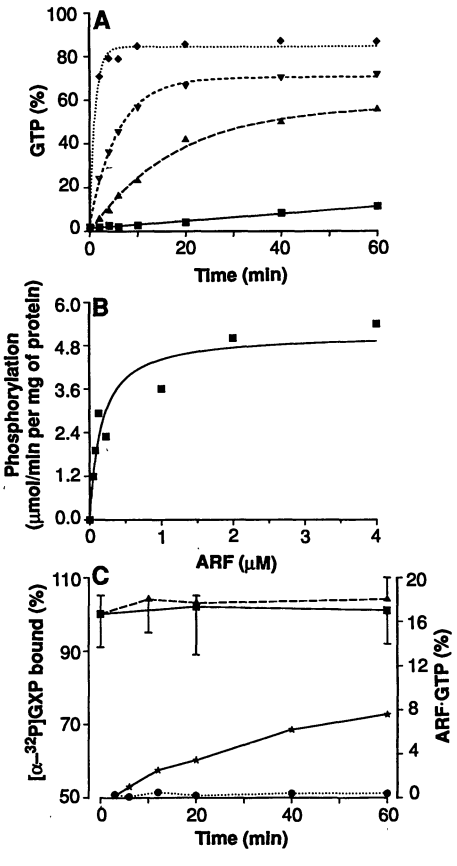

Fig. 1. NDK uses ARF·GDP as a substrate. (**A**) Rate and extent of conversion of ARF·GDP to ARF·GTP as a function of the concentration of NDK. Reaction mixtures contained 0.1 μM [α-^{32}P]GDP·ARF (*8*), 25 mM Hepes (pH 7.4), 2.5 mM $MgCl_2$, 1 mM ATP and 0 (solid squares), 1.4 nM (solid triangles), 14 nM (solid inverted triangles), or 140 nM (solid diamond) bovine liver NDK and were incubated at 30°C. At the indicated times, duplicate samples were removed and the percent of total guanine nucleotide present as GTP was quantified (*8*). The experiment is representative of three similar experiments. (**B**) Equilibrium kinetics of NDK-catalyzed phosphorylation of ARF·GDP. The indicated concentrations of unlabeled ARF and 0.02 μM [α-^{32}P]GDP·ARF were incubated with nm23-H1 NDK (6 nM). (**C**) Nucleotide exchange kinetics on ARF. To determine the extent to which GDP dissociated from ARF, 0.1 μM [α-^{32}P]GDP·ARF was incubated with 25 mM Hepes, 1 mM DTT, 1 mM ATP, 2.5 mM $MgCl_2$, and either 100 μM GDP (solid square, solid line) or 500 nM NDK and 100 μM GTP (solid triangle, dashed line). At the indicated times, ARF was separated from free nucleotide by trapping on nitrocellulose filters as described (7). The data are reported (left axis) as a percent of nucleotide (GXP refers to GDP or GTP) bound at time 0 and are from one experiment representative of three. The error bars represent the standard deviation for triplicate determinations. To determine the rate at which GTP associated with ARF, 0.5 μM recombinant ARF was incubated in the presence of 10 μM [γ-^{32}P]GTP in 25 mM Hepes (pH 7.5), either with 2.5 mM $MgCl_2$, 1 mM DTT and 1 mM ATP (solid circle, dotted line), or with 1 mM EDTA, 0.5 mM $MgCl_2$, 3 mM L-α-dimyristoyl phosphatidylcoline, sodium cholate (0.1%) and 100 mM NaCl (solid star, solid line) at 30°C, and nucleotide bound to ARF was quantitated. Data are reported as the percentage of ARF that had exchanged nucleotide (right axis).

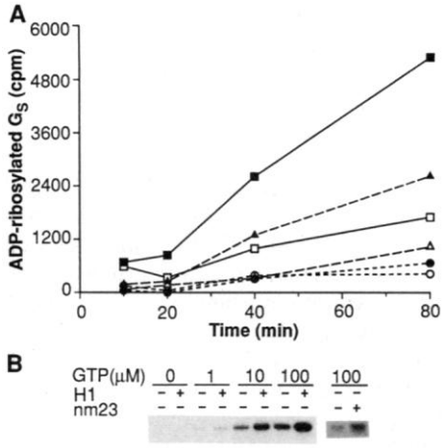

Fig. 2. Effect of NDK on cholera toxin–catalyzed ADP ribosylation of G_s. Equal concentrations (10 nM) of the proteins nm23-H1 (H1) or nm23-1 (nm23) were incubated with 25 mM Hepes (pH 7.4), 2.5 mM $MgCl_2$, 5 μM [^{32}P]NAD, 1 mM DTT, 3 mM L-α-dimyristoyl phosphatidylcholine, sodium cholate (0.1%), 1 mM ATP, 0.1 μM mARF1p, 0.05 μM recombinant $\beta_1\gamma_2$ (*19*), 0.15 μM recombinant (α_s) (*21*) α subunit of G_s and the indicated concentrations of GTP for the indicated times (A) or for 40 min (B). The [^{32}P]ADP-ribosylated G_s was separated from free NAD and quantitated either by trapping the trichloroacetic acid-precipitable material on nitrocellulose filters followed by scintillation spectroscopy (**A**) or by the addition of the sample to Laemmli sample buffer and fractionation by polyacrylamide gel electrophoresis and autoradiography (**B**) as described in (*7*). Only the 45-kD region of the gel is shown as no other bands were observed on the gels. These experiments were performed three times with similar results. Part B is a composite from two experiments with the different enzymes.

GTP even under conditions in which ARF·GTP was produced. The reaction may require binding and hydrolosis of GTP by G_s. Hydrolysis of GTP appears to be required because GTP γS cannot substitute for GTP (*15*). This conclusion is consistent with experiments showing that G_s·GTPγS is not a substrate for cholera toxin (*7*) and that point mutants of the α subunit of G_s that hydrolyze GTP slowly are poor substrates for cholera toxin (*15*).

NDK apparently phosphorylates GDP bound to ARF, which results in activation of ARF. This mechanism of activation of a regulatory GTP-binding protein obviates the need for nucleotide exchange or nucleotide exchange factors. It is not yet clear if other regulatory GTP-binding proteins can also serve as substrates for NDK. Mammalian ARF is the only regulatory GTP-binding protein without detectable intrinsic GTPase activity, although an ARF GTPase-activating protein (GAP) has been identified in bovine and yeast cells (*16*). This raises the possibility that, unlike the trimeric G proteins, activation of ARF is not the limiting step in its function in vivo. Rather, if NDK serves to maintain the ARF·GTP state, the site of regulation of the ARF signal may be the point of GTP hydrolysis, that is, interaction of ARF with the ARF GAP. Controversy exists as to whether the interaction of GAP with another small GTP-binding protein, $p21^{ras}$, serves to terminate or initiate a $p21^{ras}$ signal (*17*). ARF is an abundant coat protein on nonclathrin-coated, Golgi-derived vesicles (*18*). Thus, ARF might regulate a specific step in vesicular traffic, for example, vesicle uncoating or fusion, which would be initiated by the ARF GAP-stimulated hydrolysis of GTP on ARF at the acceptor membrane site.

REFERENCES AND NOTES

1. P. Berg and W. K. Joklik, *Nature* **172**, 1008 (1953); H. A. Krebs and R. Hems, *Biochim. Biophys. Acta* **12**, 172 (1953).
2. Y. C. Cheng, R. P. Agarwal, R. E. Parks, *Biochemistry* **10**, 2139 (1971); R. E. Parks and R. P. Agarwal, *Enzymes* **8**, 307 (1973).
3. A. M. Rosengard *et al.*, *Nature* **342**, 177 (1989); G. Bevilacqua, M. E. Sobel, L. A. Liotta, P. S. Steeg, *Cancer Res.* **49**, 5185 (1989); P. S. Steeg, *J. Natl. Cancer Inst.* **80**, 200 (1988); C. Hennessy *et al.*, *ibid.* **83**, 281 (1991); P. S. Steeg *et al.*, *Cancer Res.* **48**, 6550 (1988); A. Leone *et al.*, *Cell* **65**, 25 (1991); J. Biggs *et al.*, *ibid.* **63**, 933 (1990).
4. K. Ohtsuki, F. Ishii, M. Yokoyama, *Biochem. Int.* **11**, 719 (1985); H. Uesaka, M. Yokoyama, K. Ohtsuki, *Biochem. Biophys. Res. Commun.* **143**, 552 (1987); K. Ohtsuki and M. Yokoyama, *ibid.* **148**, 300 (1987); N. Kimura and N. Nagata, *J. Biol. Chem.* **254**, 3451 (1979); N. Kimura and N. Shimada, *ibid.* **258**, 2278 (1983).
5. S. Kikkawa *et al.*, *J. Biol. Chem.* **265**, 21536 (1990).
6. L. S. Schleiffer *et al.*, *ibid.* **257**, 20 (1982).
7. R. A. Kahn and A. G. Gilman, *ibid.* **261**, 7906 (1986).
8. Purified recombinant mamalian ARF1p (mARF1p) was prepared according to method II as described [O. Weiss, J. Holden, C. Rulka, R. A. Kahn, *J. Biol. Chem.* **264**, 21066 (1989)]. The protein was preloaded with [α-^{32}P]GDP by incubating mARF1p (~5 μM) with trace concentrations of [α-^{32}P]GDP (30 to 50 μCi at 3000 Ci/mmol) in 25 mM Hepes (pH 7.4), 1 mM EDTA, 1 mM DTT, 0.5 mM $MgCl_2$, 100 mM NaCl, 3 mM L-α-dimyristoyl phosphatidylcholine and sodium cholate (0.1%) in a total volume of 100 μL for 2 hours at 30°C. Free nucleotide was removed and buffer was exchanged on a G-25 Sephadex column equilibrated in a buffer containing 20 mM Hepes (pH 7.4), 1 mM EDTA, 2 mM $MgCl_2$, 100 mM NaCl, 1 mM dithiothreitol (DTT) and sodium cholate (1%). To determine NDK activity, [α-^{32}P]GDP or ARF that had been loaded with [α-^{32}P]GDP was incubated as described and at the indicated times samples were removed from the reaction and applied to cellulose polyethylenimine, thin-layer chromatography plates. To separate GTP from GDP, chromatograms were developed in a solution of 1 M LiCl and 1 M formic acid. Nucleotides were visualized by autoradiography and were quantified by scintillation spectroscopy.
9. The control, with no added NDK, (Fig. 1A) had a discernible rate of NDK activity because ARF was contaminated with NDK (~0.001%). Contamination of ARF, G protein, and βγ preparations is common.
10. P. A. Randazzo and R. A. Kahn, unpublished data.
11. To prepare recombinant nm23-H1, nm23-H2, and nm23-1, the coding regions were amplified by the polymerase chain reaction (PCR) with cDNAs (supplied by P. Steeg) as template and synthetic oligonucleotides that incorporate an Nde I site at the initiating methionine and a Bam HI site 6 bp downstream of the stop codon as described [R. A. Kahn *et al.*, *J. Biol. Chem.* **266**, 2606 (1990)]. The Nde I–Bam HI fragments were inserted into pET3C (supplied by W. Studier) at Nde I and Bam HI sites. BL21 (DE3) cells, were transfected with the plasmid and protein expression was induced with IPTG. The bacteria were lysed by sonication and after centrifugation (45 min at 100,000*g*), ammonium sulfate (40%) was added to the supernatant, and the resulting mixture was incubated for 1 hour at 4°C. Supernatants were then brought to 60% $(NH_4)_2SO_4$ and incubated for 1 hour at 4°C. Precipitated material was suspended in and dialyzed against 20 mM tris (pH 7.4) containing NaCl (0.9%). The dialysate was fractionated on hydroxylapatite (5 ml, Bio-Rad HTP), equilibrated in a buffer (TED) containing 20 mM tris (pH 7.4), 1 mM EDTA, 1 mM DTT. The column was washed with TED and developed with a linear gradient of 0 to 300 mM potassium phosphate (pH 7). From 1 liter of bacteria, we recovered 11, 4.3, and 23 mg of nm23-H1, nm23-H2, and nm23-1, respectively, consistent with their level of expression in BL21 (DE3) cells. Specific activities determined with deoxythymidine 5′-diphosphate as a substrate and the coupled assay [R. P. Agarwal, B. Robison, R. E. Parks, *Methods Enzymol.* **51**, 376 (1978)] were 482 U/mg, 740 U/mg, 724 U/mg, and 257 U/mg at 20°C for nm23-H1, nm23-H2, nm23-1, and Sigma enzyme N-2635 (bovine liver), respectively. The proteins were estimated to be 90% pure by staining with Coomassie blue.
12. To determine kinetic parameters, [α-^{32}P]GDP or [α-^{32}P]GDP·ARF were incubated with nm23-H1 as described in a total reaction volume of 50 μL. Samples (5 μl) were taken periodically during a 60-min incubation and nucleotides were separated and quantitated as described (*8*). The data were fitted to the single exponential model [GTP] = [GTP$_e$] (1 − e^{kt}) + *C*, and the initial rates were calculated as [GTP$_e$]*k*. The initial rates determined at seven concentrations of ARF·GDP and eight concentrations of free GDP were used for calculating K_m and V_{max} from (i) the Michaelis-Menten equation when ARF was used as a substrate and (ii) a rate equation including a term for formation of an abortive complex when free GDP was used as substrate. This latter equation was used because NDK forms an abortive complex with high concentrations of free nucleotide [N. Mourad and R. E. Parks, *J. Biol. Chem.* **241**, 271 (1966); J. Sedmark and R. Remaley, *ibid.* **246**, 53 (1971); M. G. Colomb, A. Cheruy, P. V. Vignais, *Biochemistry* **8**, 1926 (1969); A. F. Goffeau, P. L. Pedersen, A. L. Lehninger, *J. Biol. Chem.* **242**, 1845 (1967)]. The rate equation that accounts for this [E. Garces and W. W. Cleland, *Biochemistry* **8**, 633 (1969)] is

$$v = \frac{VAB}{K_aB(1 + B/K_{ib}) + K_bA(1 + A/K_{ia}) + AB}$$

Keeping one substrate concentration constant, the equation can be written as

$$v = \frac{VA}{K_{a,app} + A(1 + A/K_{ia,app})}$$

which was the equation used to derive the kinetic parameters of the H1 enzyme with free GDP. The data reported are the means ± SE determined for an experiment representative of three.
13. To measure GTP hydrolysis, [α-^{32}P]GTP (~1 μCi in 100 μl) was incubated with 25 mM Hepes (pH 7.4), 2.5 mM $MgCl_2$, 5 μM nicotinamide adenine dinucleotide, 1 mM DTT, 3 mM L-α-dimyristoyl phosphatidylcholine, sodium cholate (0.1%), 1 mM ATP, 0.1 μM mARF1p, 0.05 μM recombinant G protein βγ subunits, and 0.15 μM alpha subunit of G_s at 30°C. Aliquots (5 μl) were withdrawn and applied to cellulose polyethyleneimine (PEI) thin-layer chromatography plates. Phospholipid was removed by dipping the plates in chloroform. The nucleotides were then fractionated and quantitated as described (*8*).
14. R. A. Kahn, *J. Biol. Chem.* **266**, 15595 (1991).
15. M. P. Graziano and A. G. Gilman, *ibid.* **264**, 15475 (1989).
16. C. Rulka and R. A. Kahn, unpublished data.

17. F. McCormick, *Cell* **56**, 5 (1989).
18. T. Serafini *et al.*, *ibid.*, in press.
19. G protein βγ subunits purified from bovine brain were found to contain NDK (~0.05%) as a contaminant. Hence, recombinant βγ, which was found to have less contamination (0.001%), was used for these studies. The recombinant $\beta_1\gamma_2$ was prepared as described [D. Wildman, H. Tamir, J. K. Northup, M. Dennis, in preparation]. Briefly, Sf9 cells were co-infected with baculovirus that contained β_1 and γ_2 inserts, and the membrane-associated $\beta_1\gamma_2$ dimer was purified to homogeneity.
20. Purified recombinant α subunit from G_s (α_s) (from M. P. Graziano) was prepared as described [M. P. Graziano, P. J. Casey, A. G. Gilman, *J. Biol. Chem.* **262**, 11375 (1987); M. P. Graziano, M. Freissmuth, A. G. Gilman, *ibid.* **264**, 409 (1989).]
21. We thank R. E. Parks and P. Steeg for helpful discussions; P. Steeg for nm23-H1, nm23-H2, and nm23-1 cDNAs; R. King for nm23-H1 protein; M. Dennis for the baculovirus constructs with β_1 and γ_2 inserts; and M. Graziano for purified recombinant α_2.

7 June 1991; accepted 2 August 1991

Long-Range Structure in Ribonuclease P RNA

ELIZABETH S. HAAS,* DANIEL P. MORSE,* JAMES W. BROWN,* FRANCIS J. SCHMIDT, NORMAN R. PACE†

Phylogenetic-comparative and mutational analyses were used to elucidate the structure of the catalytically active RNA component of eubacterial ribonuclease P (RNase P). In addition to the refinement and extension of known structural elements, the analyses revealed a long-range interaction that results in a second pseudoknot in the RNA. This feature strongly constrains the three-dimensional structure of RNase P RNA near the active site. Some RNase P RNAs lack this structure but contain a unique, possibly compensating, structural domain. This suggests that different RNA structures located at different positions in the sequence may have equivalent architectural functions in RNase P RNA.

RIBONUCLEASE P (RNASE P) CLEAVES precursor tRNAs to produce the mature 5′ ends; it occurs in vivo as a complex between a small protein (119 amino acids in *Escherichia coli*) and a much larger RNA (377 nucleotides). The RNA is the catalytic moiety (*1*). It is anticipated that the three-dimensional structure of the RNA determines its binding specificity and creates the catalytic site. Using two related approaches, we have identified a structure in RNase P that places constraints on three-dimensional models. Comparisons of this structure in RNase P RNAs from different organisms point to evolutionary substitution of functional domains in RNase P RNA.

We used sequence covariation (coordinated changes in nucleotide sequences) to identify base-paired elements in RNase P RNA. In a phylogenetic approach, we compared sequences of RNase P RNAs from different organisms (*2, 3*). Base-paired elements are identified by evolutionary variations that maintain the potential for Watson-Crick pairing (A-U or G-C) (*4*). In an ongoing survey of RNase P RNAs of diverse eubacteria, we have encountered covariations in sequences found to be invariant in other studies. These new sequences are from *Streptomyces bikiniensis* var. *zorbonensis* (*5*), *Deinococcus radiodurans* (*6*), and *Thermotoga maritima* (*6*). Covarying nucleotides and the consequences of their interaction in the RNase P RNA secondary-structure model are shown in Fig. 1.

Induced mutational analysis is an alternative to phylogenetic comparisons for the identification of interacting sequences. Mutations that interfere with function were introduced into the RNase P RNA, then second-site "suppressor" mutations that restore function were identified. We considered two nucleotides to form base pairs in the RNA structure if the suppressor mutation was complementary to the original mutation. At pH 6, hydroxylamine induces unidirectional G to A or C to T changes in DNA (*7*). Therefore, two induced mutagenic events can convert a G-C base pair in RNA secondary structure into an A-U pair, allowing us to identify nucleotides that interact by Watson-Crick pairing. Defective variants of RNase P RNA were screened in *E. coli* FS101. This strain produces a defective RNase P protein, causing a temperature-sensitive growth phenotype (*8*). Introduction of a high copy-number plasmid containing a functional *rnp*B gene, which encodes RNase P RNA, allows FS101 to grow at 42°C; however, a gene coding for a sufficiently defective RNase P RNA does not suppress the temperature-sensitive phenotype (*9*).

Hydroxylamine-generated mutant plasmids that did not suppress the temperature-sensitive phenotype of FS101 were isolated and sequenced (*10*) (Fig. 1B). All of these mutant genes had acquired one or two G-C to A-T transitions. Mutant plasmids that contained single lesions were subjected to a second round of hydroxylamine treatment and introduced into FS101. We identified reverted *rnp*B genes by their restoration of the ability to support the growth of FS101 at the restrictive temperature (Fig. 2).

Our comparative and mutational data revealed base pairs (Fig. 1) in helices that form two pseudoknots (*11*) in the RNA. One of the pseudoknots results from pairing of nucleotides 82 to 85 with 276 to 279 [(helix 82-85/276-279; numbering and helix nomenclature are described in (*12*)]. The mutational data show that G82 and G83 pair with C279 and C278, respectively (Fig. 1B); phylogenetic covariations support the pairing of G82 with C279, G83 with C278, and G84 with C277 (Fig. 1A). Equivalent pairings exist in all known RNase P RNAs except those of *Bacillus*, in which the structures of the contacting domains that create the pseudoknot are different.

It has been pointed out that the simultaneous occurrence of helices 12-18/336-342 and 70-73/354-357 results in the formation of a pseudoknot in RNase P RNA (*2*). Helix 70-73/354-357 has been extended by pairing G74, thought to be paired elsewhere, with C353 (*3*). It was recognized that this helix could potentially extend another three base pairs (66-68/358-360) if U69 were bulged from the helix. However, no evidence for these pairings had been encountered (*3*). Phylogenetic (Fig. 1A) and mutational (Fig. 1B) covariations now confirm the occurrence of two of the three base pairs in that extension.

The two types of sequence covariation analysis used in this study are formally equivalent, but there are important differences in the information that can be obtained. The phylogenetic approach allows the detection of base pairs only if the appropriate covariations can be found. Some variants, however, may be rare or absent in nature. In such cases, mutagenesis is required to test the pairing. Mutagenesis, on the other hand, is limited by the availability of a sensitive assay for the biological activity of the RNA. Although complementation of FS101 appears to meet this requirement, it is likely that some mutations were not detected because they did not result in a sufficiently defective enzyme or because the mutant RNA is lethal to the host at the permissive temperature. A specific limitation of hydroxylamine mutagenesis is that only G-C base pairs can be tested.

The two pseudoknots in the RNase P

E. S. Haas, J. W. Brown, N. R. Pace, Department of Biology, Indiana University, Bloomington, IN 47405. D. P. Morse and F. J. Schmidt, Department of Biochemistry, University of Missouri–Columbia, Columbia, MO 65212.

*The first three authors and laboratories contributed equivalently to the work described in this manuscript.
†To whom correspondence should be addressed.